CURRENT STATE OF RESEARCH AT IMPERIAL COLLEGE LONDON IN RF HARVESTING AND INDUCTIVE POWER TRANSFER

Manuel Pinuela[1], D. C. Yates, S. Lucyszyn, P. D. Mitcheson

[1]Imperial College London, Electrical and Electronic Engineering Department, Optical and Semiconductor Devices Group, Exhibition Road, London, U.K. SW7 2AZ

m.pinuela09@imperial.ac.uk

Abstract: This paper presents simulation and experimental results for ambient RF energy harvesting and Inductive Power Transfer systems. End-to-end and dc-load efficiency measurements and calculations were performed to demonstrate the capabilities of both systems, respectively. An RF spectral survey was conducted across all the 270 underground stations in London. DTV, GSM900, GSM1800 and 3G were selected as the highest contributors and single banded rectennas were fabricated for all frequencies. Ground level measurements demonstrate that more than 50 stations have suitable channel power levels per band to allow ambient RF energy harvesting. Efficiencies of up to 40% were achieved with a single banded rectenna operating at GSM 900, and efficiencies higher than 20% were achieved for TV and 3G. Furthermore a high frequency, semi-resonant Class-E driver was used to transfer more than 60 W of power across a 30 cm distance with a dc-load efficiency of 72%.

Keywords: inductive power transfer, RF energy harvesting, Class-E, rectenna

INTRODUCTION

Wireless power transfer (WPT) technology, although not a new topic, has seen a recent resurgence for RF energy harvesting and inductive power transfer (IPT) [1]. This paper analyses both technologies demonstrating overall system efficiencies for ambient energy harvesting and IPT. Only a few attempts have been made to harvest ambient energy from multitone, non-dedicated sources, as shown by [2]. Therefore, the challenge is to design a rectenna capable of harvesting energy from true ambient sources and provide useful amounts of power to the specified load. To achieve this, measurement results from an ambient RF spectral survey covering 270 underground stations in London were used to design four single banded rectennas capable of harvesting ambient energy.

IPT systems with link efficiencies as high as 95%, driven by standard signal generators or RF transmitters have previously been presented [3]. In these analyses, the end-to-end and dc-load efficiency of the system is usually omitted and therefore a clear understanding of the overall system performance remains unknown. Here we provide an overall system analysis and will show measurement results for an IPT link driven by a tuned semi-resonant Class-E driver across different separation distances.

LONDON RF SURVEY

Miniature RF harvesters require small antennas and hence ambient frequencies in the range of 300-3000 MHz are of interest for harvesting. In order to assess the ambient urban power levels of such signals, an RF spectral survey was performed at each of the 270 London underground stations. An Agilent FieldFox RF analyser and a calibrated Aaronia omnidirectional antenna using well established methodologies, such as the "panning approach" approved by the ECC [4]. This technique was used to measure the maximum field strength values after sweeping across the three axes. To increase the signal-to-noise ratio (SNR) and the sensitivity of the measurements, the minimum attenuation level was selected, while avoiding measurement compression when high input power levels were detected.

The data that was acquired during measurement gives insight into which London locations and scenarios are suitable for placing RF harvesters. Time, location, field strength, power density and channel power analysis are available at the London RF Survey website www.londonrfsurvey.org [5].

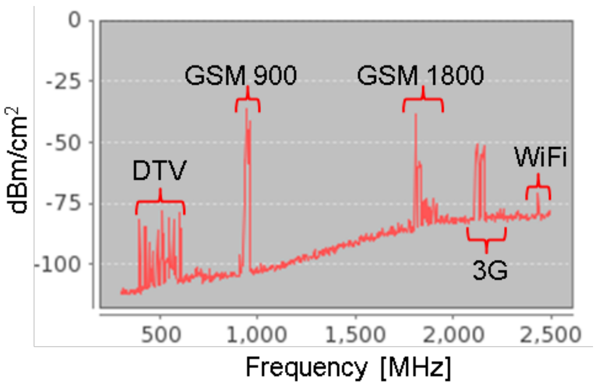

Fig. 1. Northfields station power density measurement.

Fig. 1 shows the power density measurement outside Northfields London underground station, at street level. Peaks can be identified for digital TV (DTV), GSM 900, GSM 1800, 3G and WiFi frequency bands. As will be demonstrated in the next section, the power levels available at Northfields station, as well as more than 50 other survey locations, are high enough to be efficiently harvested.

Band name	Frequency (MHz)	Average P (μW/cm^2)	Maximum P (μW/cm^2)
DTV	470 - 610	0.0034	0.023
GSM 900	921 - 960	0.014	0.54
GSM 1800	1805 - 1876	0.01	0.49
WiFi	2400 - 2473	0.009	0.02
3G	2110 - 2170	0.02	0.13

Table 1. London RF survey measurement summary.

Table 1 presents a summary of the results gathered from the RF spectral survey, where P is the power density. It was concluded that DTV was heavily dependent on atmospheric conditions [6] and WiFi was heavily dependent on traffic, making the latter intermittent as a source for energy harvesting. Finally DTV, GSM 900, GSM 1800 and 3G were identified as the frequency bands with the highest power density levels across London.

SINGLE-BAND HARVESTERS

Based on the spectral survey measurements and the available power levels (around -20 dBm = 10 µW of channel power per band, in some locations), the Skyworks SMS7630 zero bias Schottky diode detector in a half-wave series diode configuration was selected as the most suitable rectenna topology [7]. Harmonic balance simulations were conducted using Agilent ADS™, to account for the non-linear behaviour of the detector, and full-wave 3D electromagnetic simulator CST™ were performed to simulate an easy to scale and fabricate, folded dipole omnidirectional antennas. Both a 0.56 mm diameter wire antenna and a flat copper antenna were fabricated for each harvester.

The RF harvester was designed and fabricated on low-cost FR4 substrate for each of the selected bands. Impedance matching was achieved for Zo = 50 Ω with a lumped-element impedance matching network.

A state-of-the-art, low power integrated circuit from Texas Instruments was selected for the power processing module. The BQ25504 is a boost converter, with built-in maximum power point tracking (MPPT) and battery management, capable of working at microwatt power levels. It consumes a quiescent current of less than 330 nA and operates with an input voltage as low as 80 mV. To program the BQ25504 to achieve good MPPT operation, measurements of the maximum power point to open circuit voltage were performed. The ratio was between 0.48 to 0.53 for the four harvesters with either a wire or flat antenna.

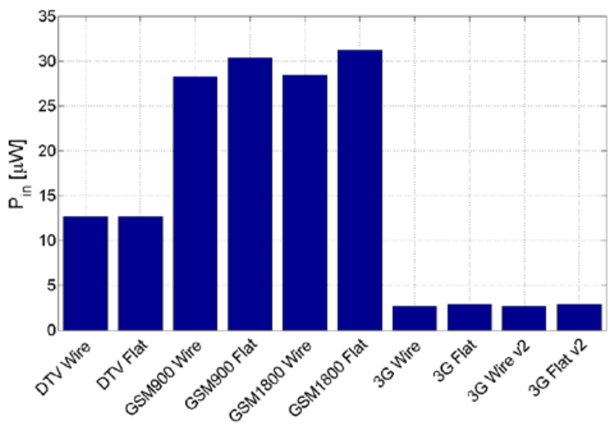

Fig. 2. Integrated available power per band at the input of the detector for wire and flat antenna.

To calculate the integrated available power, P_{in}, from the measured power density P [µW/cm^2], (1) was used.

$$P_{in} = P\frac{\lambda^2 G}{4\pi} \quad (1)$$

where λ is the wavelength of the centre frequency (fo) of each band, G is the maximum simulated antenna gain at fo. Fig. 2 shows the integrated available power per band of measurements taken in the EEE Department at Imperial College London. Furthermore, equations (2), (3) and (4) were used to calculate the end-to-end efficiency, η_{e-e}.

$$E_{in} = P_{in}\left(t_{cycle}\right) \quad (2)$$

$$E_{out} = \frac{C_{stor}\left(V_{batOK}{}^2 - V_{batLOW}{}^2\right)}{2} \quad (3)$$

$$\eta_{e-e} = \frac{E_{in}}{E_{out}} \quad (4)$$

where, t_{cycle} is the charge-discharge cycle time of the storage capacitor, C_{stor}, V_{batOK} and V_{batLOW} are 2.8 V and 2.4 V respectively and E_{in} and E_{out} is the input and output energy, respectively.

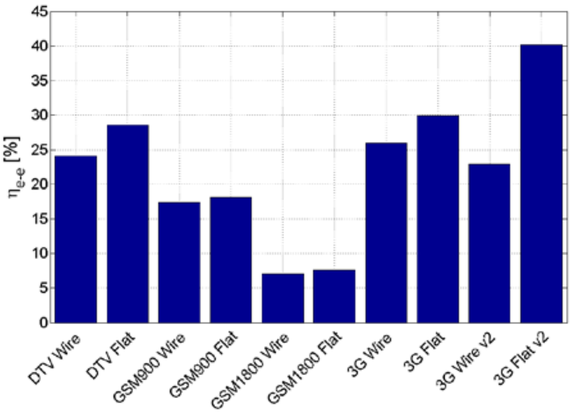

Fig. 3. End-to-end harvester efficiency per band measured at Imperial College London.

A second version of the 3G harvester was prototyped using a distributed matching network and a quarter wavelength stub, to filter higher order harmonics. As can be seen in Fig. 3, the second version rectenna (3G v2), with simplified matching network and Zo = 92 Ω, proved to be considerably more efficient, achieving an end-to-end efficiency of 40% (15% higher than the lumped-element matching network version).

These results together with the city-wide spectral survey prove that ambient RF energy harvesting for low power, duty-cycled application can be genuinely realized in an urban scenario.

IPT COIL DESIGN AND DRIVER

At Imperial College London, we are also working in an IPT system capable of transmitting tens to hundreds of Watts at close proximity, as an alternative to far-field RF power transfer. An inductive power transfer system is comprised of, but not limited to: dc power supply unit and driving clock for power amplifier, power amplifier, impedance matching network, transmitting and receiving coils, rectifier and a load. To analyse all of these blocks and characterize the IPT system in its entirety, the end-to-end efficiency η_{ee} from the ac source to the load needs to be considered as follows:

$$\eta_{ee} = \eta_{dcPSU}\eta_{dc-load} \quad (5)$$
$$\text{where } \eta_{dc-load} = \eta_{driver}\eta_{link}$$
$$\text{and } \eta_{dc-load} = \frac{P_{load}}{P_{dc}}$$

where η_{dcPSU} is the efficiency of the dc power supply, $\eta_{dc\text{-}load}$ is the dc-load efficiency, η_{driver} is the efficiency of the driver, η_{link} is the link efficiency, η_{clock} is the efficiency of the driver clock, η_{amp} is the efficiency of the amplifier. This paper will focus in the analysis of $\eta_{dc\text{-}load}$ of an IPT system without taking into account the efficiency of the dc power supply unit, where P_{dc} is the total dc input power to the system and P_{load} is the average power dissipated in the load. Since the load consists of an array of resistors, a rectifier not included in the design and will be added in future work to demonstrate the system's capability of suppling energy to a wireless sensor node and an electric vehicle.

A consistent figure of merit, such as $\eta_{dc\text{-}load}$ and η_{ee}, should be used to evaluate IPT systems; to allow a straightforward comparison of the different emerging technologies in this field. As can be clearly appreciated from the latter figure and equations, the link efficiency describes just part of the system's efficiency and does not take into account the driver, whose inefficiency can be significant. The challenge here is to realise a high frequency, cost effective and efficient solution for mid-range IPT in the absence of coupling enhancing techniques, in order that the system is tolerant to misalignment. The system must be able to achieve high efficiency for lower coupling factors, due to a smaller receiver coil size. The transmitter (TX) and receiver (RX) coil size difference represents a more realistic system, where the receiver size is usually constrained by its embodiment.

A. Class-E design

Based on the coil design considerations and Q-factor measurements techniques presented in [8], simulated and measured values of an unloaded Q = 1,100 for the 5-turn, 20 cm diameter RX coil and Q = 1,270 for the 3-turn, 30 cm TX coil were achieved. Based on these results, the operating frequency for the IPT system was selected to be 6 MHz.

To achieve a better match between driver simulations and measurements, coupling factor k measurements were undertaken to characterize the coil coupling in an array of different scenarios that will be presented in future work [9]. Measurements were undertaken with different separation distances, as illustrated in Fig. 4. Data from these measurements was also used to predict the operating characteristics, as well as the expected efficiency of the IPT system. The k measurements and calculations were performed with a well-known voltage transfer technique, as described in detail in [10].

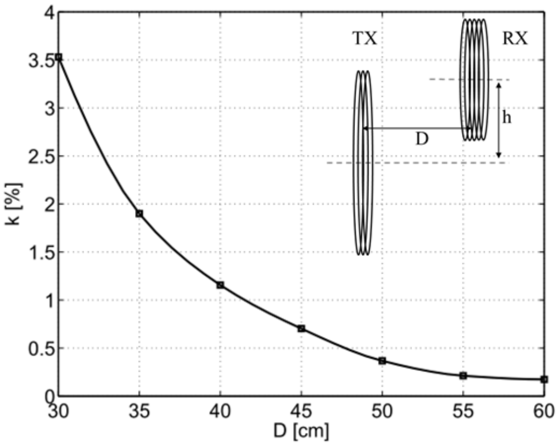

Fig. 4. k vs. D measurements for perfectly aligned coils.

In order to avoid the inherent losses present in a typical coil driver system, consisting of a 50 Ω loop that is impedance matched to a high frequency RF transmitter, a semi-resonant Class-E driver, as introduced in [10], was designed. The use of a driver specifically designed based on the transmitting and receiving coil characteristics provides an efficient way of achieving not only high link efficiencies (95% based on Q and k measurements) but also high dc-load efficiencies. This is due to the fact that with a non 50 Ω driving system, the coils do not have to be impedance matched for maximum power transfer; therefore a design that optimises the dc-load efficiency can be accomplished.

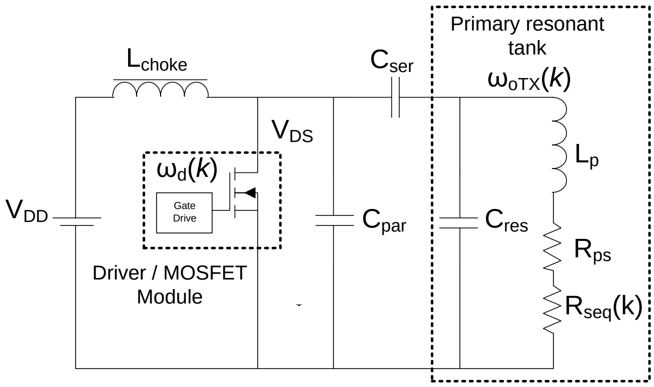

Fig. 5. Semi-resonant Class-E topology.

In this coil driver topology, the effective load resistance (composed of the transmitter coil series resistance R_{ps} and the effective receiver resistance $R_{seq}(k)$) and transmitter coil inductance L_p, appear to be larger, thus helping to increase both driver and link efficiencies. This is achieved by tuning the loaded transmitter resonant tank to a higher driven resonant frequency $\omega_{oTX}(k)$ than the receiver resonant tank driven resonant frequency $\omega_{oRX}(k)$, at which the MOSFET gate driver switches at an operating frequency $\omega_d(k) = 1/T$, as shown below:

$$\omega_{oTX}(k) > \omega_{oRX}(k) \equiv \omega_d(k) \qquad (6)$$

The IXZ421DF12N100 integrated driver/MOSFET module was selected as the best solution due to its high power handling and nanosecond switching capabilities. This module was also selected due to its relatively low output capacitance at a drain-source voltage V_{DS} = 230 V required for driving more than 100 W.

After tuning the Class-E to achieve zero current and zero voltage switching, dc-load efficiency measurements were performed for a variable separation distance. Since the Agilent N2783A current probes are incapable of measuring accurately with the presence of significant electromagnetic noise, and the fact that the "non-inductive" resistors used as the resistive load (21 kΩ) had a relatively large parasitic shunt capacitance of 2.8 pF at 6 MHz, an indirect temperature measurement was used, as follows:

$$\eta_{dc-load} = \frac{\dfrac{T_{ssRX} - T_{amb}}{\theta_{sink}}}{P_{dc}} \qquad (7)$$

where T_{ssRX} is the heat sink steady-state temperature of the receiver coil, T_{amb} is the ambient temperature, θ_{sink} is the thermal resistance of the heatsink and P_{dc} is the electrically measured total input dc power into the system. This measurement technique provides a good approximation of the dc-load efficiency, where all the dissipated power is assumed to flow through θ_{sink} due to its very low value compared to the other thermal paths, as the junction-to-case thermal resistance of the TO-220 resistor package.

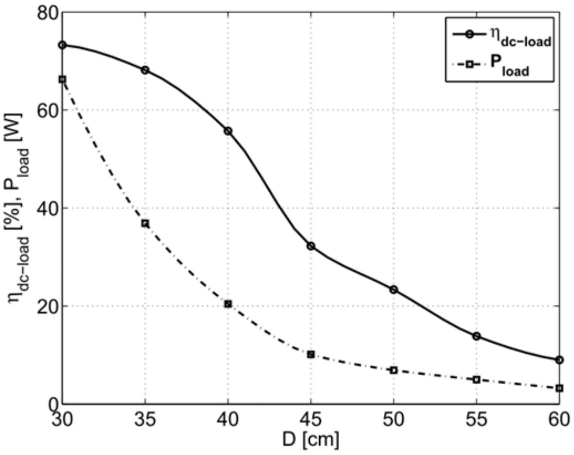

Fig. 6. DC-load efficiency measurements for different separation distances optimized for D=30 cm.

Fig. 6 shows the measured dc-load efficiency for a perfectly aligned IPT system while coil separation, *D*, varies with a fixed impedance tuning optimized for 30 cm. As can be appreciated from this figure, dc-load efficiencies above 50% were achieved for coil separation distances up to 42 cm and a maximum dc-load efficiency of 72% was achieved with a separation distance of 30 cm, while 68 W were dissipated in the resistive load.

CONCLUSIONS

A number of single-band RF ambient energy harvesters were designed and fabricated proving, together with a city-wide RF spectral survey, that ambient RF energy harvesting is a realizable technology. Also, a high frequency IPT system capable of achieving a dc-load efficiency of 72% at a separation distance of 30 cm and efficiencies above 50% for even larger separation distances were presented. Further analysis on both technologies will be presented in future publications.

ACKNOWLEDGMENTS

The authors would like to thank Georgios Pappas for his help during experiments, the UK government, CONACYT (Mexican National Council of Science and Technology) and the European Community's Seventh Framework Program under grant agreement No. 223975, Project MOBESENS for the partial funding of this work. Also, IXYSRF and Dielectric Laboratories for providing useful advice and component samples.

REFERENCES

[1] N. Shinohara, 'Power without wires', *IEEE Microwave Magazine*, vol. 12, no. 7, p. S64–S73, Dec. 2011.

[2] C. Mikeka, H. Arai, A. Georgiadis, and A. Collado, 'DTV band micropower RF energy-harvesting circuit architecture and performance analysis', in *2011 IEEE International Conference on RFID-Technologies and Applications (RFID-TA)*, 2011, pp. 561–567.

[3] S. H. Lee and R. D. Lorenz, 'Development and Validation of Model for 95% Efficiency, 220W Wireless Power Transfer over a 30cm Air-gap', *IEEE Transactions on Industry Applications*, vol. PP, no. 99, p. 1–1, 2010.

[4] 'CEPT.ORG - ECC'. [Online]. Available: http://www.cept.org/ecc. [Accessed: 12-Mar-2012].

[5] 'London RF Survey'. [Online]. Available: http://londonrfsurvey.org/. [Accessed: 22-May-2012].

[6] J. C. Whitaker, *The Rf Transmission Systems Handbook*. CRC Press, 2002.

[7] M. Pinuela, P. D. Mitcheson, and S. Lucyszyn, 'Analysis of Scalable Rectenna Configurations for Harvesting High Frequency Ambient Radiation', in *Proceedings of PowerMEMS 2010*, Leuven, Belgium, 2010.

[8] M. Pinuela, D. C. Yates, P. D. Mitcheson, and S. Lucyszyn, 'Maximising the Link Efficiency of Resonant Inductive Coupling for Wireless Power Transfer', presented at the 1st International Workshop on Wireless Energy Transport and Harvesting, Eindhoven, The Netherlands, 2011.

[9] M. Pinuela, D. C. Yates, S. Lucyszyn, and P. D. Mitcheson, 'Maximising DC-load efficiency for semi-resonant inductive power transfer', *In preparation for IEEE Transactions on Power Electronics*.

[10] K. V. Schuylenbergh and R. Puers, *Inductive Powering: Basic Theory and Application to Biomedical Systems*. Springer, 2009.